

Conversion of low-density polyethylene into carbon nanotubes for catalytic activation of persulfate and degradation of water organic micropollutants

Octávia Vieira¹, Rui S. Ribeiro^{1,*}, Fernanda F. Roman^{1,2}, Jose L. Diaz de Tuesta^{2,*}, Adrián M.T. Silva¹, Helder T. Gomes²

¹ *Laboratory of Separation and Reaction Engineering - Laboratory of Catalysis and Materials (LSRE-LCM), Faculdade de Engenharia, Universidade do Porto, Rua Dr. Roberto Frias, 4200-465 Porto, Portugal.*

² *Centro de Investigação de Montanha (CIMO), Instituto Politécnico de Bragança, Campus de Santa Apolónia, 5300-253 Bragança, Portugal.*

* Corresponding authors. E-mail addresses:

rsribeiro@fe.up.pt (Rui S. Ribeiro); jl.diazdetuesta@ipb.pt (Jose L. Diaz de Tuesta)

This article has been accepted for publication and undergone full peer review.
Please cite this article as DOI: 10.1016/j.jenvman.2022.114622.

Abstract

Plastic derived carbon nanotubes (CNTs) were tested as catalysts in persulfate activation for the first time. Four catalysts were prepared by wetness impregnation and co-precipitation (using Al₂O₃, Ni, Fe and/or Al) and implemented to grow CNTs by chemical vapour deposition (CVD) using low-density polyethylene (LDPE) as carbon feedstock. A catalyst screening was performed in batch mode and the best performing CNTs (CNT@Ni+Fe/Al₂O₃-cp) led to a high venlafaxine mass removal rate (3.17 mg g⁻¹ h⁻¹) in ultrapure water after 90 min (even with a mixture of micropollutants). Its degradation increased when the matrix was replaced by drinking water and negligibly affected in surface water. A composite polymeric membrane was then fabricated with CNT@Ni+Fe/Al₂O₃-cp and polyvinylidene fluoride (PVDF), a high venlafaxine mass removal rate in surface water being also observed in 24 h of continuous operation. Therefore, the results herein reported open a window of opportunity for the valorisation of plastic wastes in this catalytic application.

Keywords: waste management; chemical vapour deposition (CVD); advanced oxidation processes (AOPs); composite polymeric membranes; contaminants of emerging concern (CECs).

1. Introduction

One of the main constraints hindering the intensification of plastic recycling practices is the lack of economic attractiveness of the resulting products (Miranda et al., 2020). At the same time, one of the main challenges of industrial-scale production of carbon nanotubes (CNTs) by catalytic chemical vapour deposition (CVD) is still its cost (Bazargan and McKay, 2012; Serp et al., 2003). In CVD, nucleation and growth of CNTs usually occur at the surface of metal catalyst particles upon decomposition of a pure hydrocarbon gas under high temperature

(typically in the range 700 – 950 °C), followed by a purification step to remove the attached catalyst particles (Lehman et al., 2011; Oberlin et al., 1976). Therefore, it comes as no surprise the fast growth in the number of research studies conducted to explore the potential synergies arising from the use of plastics as feedstock to produce CNTs. The hypothesis raised in those studies is that the stream of a pure hydrocarbon gas (*e.g.*, methane, acetylene, benzene), typically used as carbon source to feed the CVD system, can be replaced by the hydrocarbon gases released upon thermal decomposition of (low-cost) plastic wastes. In this way, the costs associated with CNTs production by catalytic CVD are expected to decrease. Moreover, the use of plastic wastes to produce added-value materials, such as CNTs, is expected to increase the economic attractiveness of plastics recycling. Therefore, the cost-effective, environmentally-friendly, and sustainable production of CNTs is expected to be achieved through this approach (Zhuo and Levendis, 2014).

The current trend towards the synthesis of CNTs from plastics is reflected in the increasing number of research articles (*cf.* Figure S1a) and in the nine review articles published since 2012 (Bazargan and McKay, 2012; Nyakuma and Ivase; Okan et al., 2019; Papari et al., 2021; Sharma and Batra, 2020; Utetiwabo et al., 2020; Wang et al., 2020; Williams, 2021; Zhuo and Levendis, 2014). Most of the original research studies on this topic are solely focused on the optimization of the synthesis conditions (>75%, *cf.* Figure S1b). Nevertheless, some articles also report the application of the resulting CNTs, namely in electrochemical and energy (Cai et al., 2020a; Cai et al., 2020b; Gao et al., 2018; Moo et al., 2019; Pol and Thackeray, 2011; Sridhar and Park, 2020; Veksha et al., 2020; Wen et al., 2014), environmental (Deokar et al., 2017; Gong et al., 2014; Sridhar and Park, 2020), composite filling (Borsodi et al., 2016; Wu et al., 2016) and nanomedicine (Mezni et al., 2017) applications. Although CNTs produced by CVD with pure hydrocarbons have been shown to be suitable materials for several advanced oxidation processes - AOPs (Duan et al., 2018), such as activated persulfate oxidation (Chen et

al., 2018) and catalytic wet peroxide oxidation (Ribeiro et al., 2016b), the environmental applications of CNTs produced from plastics are still limited to adsorption of oils (Gong et al., 2014) and organic micropollutants (MPs) (Deokar et al., 2017; Sridhar and Park, 2020), and have not been tested yet in AOPs, such as persulfate activation.

The characteristics of CNTs produced by catalytic CVD depend on the operating conditions (*e.g.*, temperature, time, pressure, etc.), and the nature and load of both hydrocarbon gas (carbon source) and metal catalyst (Szabó et al., 2010; Tessonier et al., 2009). Having all this in mind, in this work four metal catalysts were prepared from Al₂O₃, Ni, Fe and/or Al by using wetness impregnation or co-precipitation methods and employed for the growth of CNTs using low-density polyethylene (LDPE) as carbon feedstock. The resulting CNTs were characterized and used in activated persulfate oxidation experiments for the degradation of organic MPs in batch mode. Aqueous solutions of venlafaxine (250 µg L⁻¹) alone, and in mixture with atenolol, metoprolol and citalopram (250 µg L⁻¹ of each), were used as model systems of organic MPs. Venlafaxine is an antidepressant drug included during the most recent revision of the Watch List of contaminants of emerging concern (CECs) (EU Commission, 2020). The beta-blockers atenolol and metoprolol, and the antidepressant citalopram, have been detected in the environment during monitoring programmes carried out by our group, the reason why they were selected for this study (Barbosa et al., 2018; Sousa et al., 2020). Sodium persulfate was employed as oxidizing agent source.

The effect of the water matrix on the treatment performance was also studied, upon employing drinking water (DW) and surface water (SW), in addition to ultrapure (UP) water; and scavenging tests, in the presence of methanol (MeOH) and furfuryl alcohol (FFA), were performed to infer about the main oxidation species involved in the process. The best performing sample of CNTs was included as active catalytic phase in a poly(vinylidene fluoride) (PVDF) matrix by adapting a methodology previously reported by our group for the

fabrication of nitrogen-doped reduced graphene oxide – PVDF nanocomposite membranes (Vieira et al., 2020). Activated persulfate oxidation experiments for the degradation of venlafaxine in SW (at a concentration of $100 \mu\text{g L}^{-1}$) were then performed in continuous mode of operation (during 24 h) with the resulting composite polymeric membrane, as proof of concept. To the best of our knowledge, CNTs produced from plastics are herein employed for the first time in activated persulfate oxidation for the removal of organic MPs.

2. Experimental procedure

2.1. Materials, chemicals and water matrices

Al_2O_3 (particle size = 53-106 μm , BASF) was used as support for the preparation of catalysts used in the CVD process. Impregnation and co-precipitation were performed using $\text{Ni}(\text{NO}_3)_2 \cdot 6\text{H}_2\text{O}$ (99 wt.%), $\text{Fe}(\text{NO}_3)_3 \cdot 9\text{H}_2\text{O}$ (98 wt.%) and/or $\text{Al}(\text{NO}_3)_3 \cdot 9\text{H}_2\text{O}$ (99 wt.%) supplied by VWR Chemicals. NH_4OH (25%), used for precipitation, was provided by Panreac. Low-density polyethylene (LDPE; $d = 0.91 \text{ g cm}^{-3}$, average MW = $35,000 \text{ g mol}^{-1}$, in powder form) obtained from Aldrich Chemistry was used as carbon precursor for the growth of CNTs by catalytic CVD.

Venlafaxine hydrochloride, atenolol, metoprolol tartrate and citalopram hydrobromide (analytical standards), and furfuryl alcohol (FFA; 98 wt.%) were obtained from Sigma-Aldrich. Sodium persulfate (SPS; 99 wt.%) and methanol (MeOH; 99.9 wt.%) were supplied by Riedel-de Haen and Fisher Scientific, respectively. N,N-diethyl-p-phenylenediamine (DPD; 99 wt.%), sodium hydrogen phosphate (99 wt.%), sodium dihydrogen phosphate (99 wt.%) and sulfuric acid (95 wt.%) from Fluka were used for the determination of SPS. Formic acid (99 wt.%) and acetonitrile (HPLC grade), purchased from Fisher Scientific, were used to prepare the mobile phase needed for the determination of atenolol, metoprolol, venlafaxine and citalopram by high-performance liquid chromatography (HPLC).

Polyvinylpyrrolidone (PVP; MW: 40,000 g mol⁻¹), 1-methyl-2-pyrrolidone (NMP; 99.5 wt.%) and poly(vinylidene fluoride) (PVDF; MW: 275,000 g mol⁻¹), from Sigma-Aldrich, were used for membrane fabrication. All the materials and chemicals were used as received.

Ultrapure water (UP; pH = 5.9) was obtained in a Milli-Q® water purification system (Merck). Drinking water (DW; pH = 6.8) was obtained from a bottle of the commercial brand Fastio. Surface water (SW; pH = 7.5) was collected nearby the admission point of a drinking water treatment plant located in the district of Porto, Portugal, filtered (0.45 µm cellulose filters) and kept at 4 °C until use.

2.2. Preparation of the catalysts employed in CVD

Four metal catalysts were prepared from Al₂O₃, and Ni, Fe and Al nitrate salts by wetness impregnation (wi) and co-precipitation (cp).

Ni/Al₂O₃-wi was prepared by wetness impregnation of Al₂O₃ with a Ni(NO₃)₂ solution (1.35 mol L⁻¹), considering 20 wt.% of NiO over Al₂O₃. Impregnation took place in a lab rotary evaporator R-114 (Buchi) at 70 °C and 72 mbar during *ca.* 3 h. Ni+Fe/Al₂O₃-wi was prepared through the same impregnation procedure, except that Ni(NO₃)₂ and Fe(NO₃)₃ solutions (0.42 and 0.87 mol L⁻¹, respectively) were employed as metal precursors.

Ni+Fe/Al₂O₃-cp was obtained by co-precipitation of Ni and Fe over Al₂O₃. For that purpose, 6.28 g of Al₂O₃ was added to a solution containing 0.027 and 0.054 mol L⁻¹ of Ni(NO₃)₂ and Fe(NO₃)₃, respectively. Afterwards, a NH₄(OH) solution (1 mol L⁻¹) was added dropwise using a peristaltic pump, under constant vigorous stirring until pH 8 was reached. Possible residues of the precursors were then washed-out with distilled water by centrifugation. Ni+Fe+Al-cp was prepared through the same co-precipitation procedure, except that an Al(NO₃)₃ solution (0.22 mol L⁻¹) was added instead of Al₂O₃.

Regardless of the synthesis procedure (*i.e.*, wetness impregnation or co-precipitation), the resulting materials were dried overnight in oven at 60 °C and subsequently calcined in static air

atmosphere (Thermolyne 6000 Furnace), at the same temperature as that employed in CVD (850 °C), during 3 h.

2.3. Preparation of CNTs

CNTs were prepared by catalytic CVD, in a Termolab vertical tubular furnace (*i.d.* = 50 mm, *L* = 500 mm) with two heating zones controlled independently by EPC3000 controllers (*cf.* Figure S2). Briefly, a crucible containing 5 g of the LDPE used as carbon feedstock was held in the top heating zone (450 °C) and 1 g of one of the four metal catalysts (prepared as described in Section 2.2) was placed on a crucible held in the bottom heating zone (850 °C). For that purpose, the bottom zone was heated at 20 °C min⁻¹ until 400 °C, and then the top and bottom zones were heated up to 450 and 850 °C, respectively, also at 20 °C min⁻¹. The simultaneous thermal decomposition of the polymer (top zone) and catalytic CVD (bottom zone) was then allowed to proceed under a N₂ flow (100 cm³ min⁻¹) for 1 h. Afterwards, the resulting solids were collected from the bottom zone, purified with 50 vol% H₂SO₄ at 140 °C during 3 h, thoroughly washed with distilled water and dried overnight in oven at 60 °C. The resulting materials were denoted as CNT@ followed by the description of the metal catalyst used for their growth by CVD, namely: CNT@Ni/Al₂O₃-wi, CNT@Ni+Fe/Al₂O₃-wi, CNT@Ni+Fe/Al₂O₃-cp, and CNT@Ni+Fe+Al-cp.

2.4. Fabrication of composite polymeric membranes

The composite polymeric membranes were obtained by including CNT@Ni+Fe/Al₂O₃-cp within a PVDF matrix, by adapting the procedure previously described (Vieira et al., 2020). For that purpose, 3.2 wt.% of powder CNT@Ni+Fe/Al₂O₃-cp was added to the membrane-forming materials, as detailed in Text S1. The resulting composite membrane was denoted as CNT@Ni+Fe/Al₂O₃-cp-PVDF and used in activated persulfate oxidation experiments performed in continuous mode of operation.

2.5. Characterization techniques

Scanning electron microscopy (SEM) images were obtained using a FEI Quanta 400FEG ESEM/EDAX Genesis X4Minstrument equipped with an Energy Dispersive Spectrometer (EDS). TEM images were obtained using a JEOL 2100, LaB6 filament, transmission electron microscope operating at 200 kV.

Textural properties, namely specific surface area calculated by the Brunauer, Emmett and Teller (BET) method (S_{BET}), and total pore volume (V_{Total}), were determined by N₂ physisorption, as previously described (Silva et al., 2019). The concentration of acidic sites at the surface of the materials was determined using the titration technique previously described (Gomes et al., 2010). The pH at point of zero charge (pH_{PZC}) was obtained by pH drift tests, as described elsewhere (Ribeiro et al., 2016a). The content of Al, Ni, and/or Fe in the CNTs was determined by inductively coupled plasma optical emission spectrometry (ICP-OES) analysis of the solution resulting from the acidic digestion of the solids, performed as described elsewhere (Ribeiro et al., 2016a).

2.6. Activated persulfate experiments

Activated persulfate experiments were performed in batch and continuous mode of operation, both at room temperature (22 ± 2 °C) and without pH adjustment. The powder CNTs prepared as described in Section 2.3 were used in the experiments performed in batch mode, while experiments in continuous mode were performed with the composite polymeric membrane (CNT@Ni+Fe/Al₂O₃-cp-PVDF) obtained as described in Section 2.4.

Experiments in batch mode were conducted in a stirred amber glass bottle loaded with 50 mL of an aqueous solution containing the model pollutant(s). In each run, a calculated amount of SPS was added to obtain the desired concentration of oxidant source (250 mg L⁻¹). After homogenization, the reaction started with the addition of the powder catalyst (0.05 or 0.25 g L⁻¹). Samples were periodically withdrawn, filtered (0.2 μm PTFE syringe filters) and kept at 4

°C until analysis. Adsorption and non-catalytic (blank) experiments were performed in the absence of SPS and catalyst, respectively. Two model systems of aqueous pollutants were considered, namely: (i) venlafaxine ($250 \mu\text{g L}^{-1}$); and (ii) a mixture containing atenolol, metoprolol, venlafaxine and citalopram ($250 \mu\text{g L}^{-1}$ of each). An additional experiment with metoprolol ($250 \mu\text{g L}^{-1}$) was conducted. Ultrapure (UP), drinking (DW) and surface (SW) water were employed as aqueous matrices in the experiments performed with venlafaxine as model system. Moreover, activated persulfate experiments were performed in the presence of methanol (MeOH) and furfuryl alcohol (FFA).

Experiments in continuous (dead-end) mode were performed using the experimental setup depicted in Figure S3. In this case, a stirred amber glass bottle was loaded with 250 mL of SW spiked with venlafaxine ($100 \mu\text{g L}^{-1}$). A calculated amount of SPS was then added to obtain the desired concentration of oxidant source (250mg L^{-1}). After homogenization, the solution was continuously fed to the glass cell containing the CNT@Ni+Fe/Al₂O₃-cp-PVDF membrane (effective area = 2.1cm^2) at a flow rate of 0.1mL min^{-1} for 24 h. Samples were periodically withdrawn and kept at 4 °C until analysis. An adsorption experiment was performed in the absence of SPS.

2.7. Analytical techniques

The concentrations of atenolol, metoprolol, venlafaxine and citalopram were determined by ultra-high-performance liquid chromatography (UHPLC) coupled with a fluorescence detector (FD), as previously described (Vieira et al., 2020). The autosampler and oven temperatures were kept at 15 and 30 °C, respectively. The mobile phase, consisting of a 77:23 volumetric mixture of an aqueous formic acid solution (0.1 vol%) and acetonitrile, was delivered at a flow rate of 0.25mL min^{-1} . The injection volume was 30 μL , and the excitation and emission wavelengths of the FD were 230 and 300 nm, respectively. Daily calibration was conducted by

analysing 10 standard solutions obtained by step dilutions of stock solutions (10.1 mg L^{-1}) prepared in ultrapure water. A summary of the method parameters is provided in Table S1.

The concentration of SPS was determined by a colourimetric method with N,N-Diethyl-p-phenylenediamine sulphate (DPD), as previously described (Vieira et al., 2020). Dissolved Fe and Ni contents were determined by ICP-OES.

3. Results and discussion

3.1. CNTs characterization

The four metal catalysts prepared from Al_2O_3 , Ni, Fe and/or Al by wetness impregnation and co-precipitation, as described in Section 2.2, were employed in the CVD system (*cf.* Section 2.3), to promote the growth of four different samples of CNTs from the LDPE feedstock. Synthesis yields in the range 15 – 20 and 7 - 16 wt.% (in respect to the mass of LDPE fed to the system) were obtained before and after purification with H_2SO_4 , respectively. Indeed, the CNTs obtained after the purification step (implemented to remove attached metal species arising from the CVD system) exhibit negligible residual metal contents (in the range 0.1 – 0.15 wt.%; *cf.* Table S2). The exception is CNT@Ni/ Al_2O_3 -wi, which reveals a higher metal content (1.24 wt.%), corresponding to Ni (0.92 wt.%) and Al (0.32 wt.%) from the CVD catalyst employed in the synthesis process. The resulting samples of CNTs were also characterized by SEM-EDS, TEM, N_2 physisorption, acid-base properties, and pH_{PZC} .

SEM micrographs confirm the growth of carbon filaments by CVD over all the prepared metal catalysts (*cf.* Figure 1), allowing to conclude about the feasibility of employing LDPE as carbon feedstock in the proposed system. As observed, long carbon filaments are obtained regardless of the catalyst employed. Nevertheless, their properties are expected to depend on the nature of the catalyst (Szabó et al., 2010; Tessonnier et al., 2009). This is the case of the external diameter determined by SEM, which was in the range 4 – 63 nm. Higher external

diameters were obtained in the carbon materials prepared over the two Ni+Fe/Al₂O₃ supported catalysts (prepared by wetness impregnation and co-precipitation), namely CNT@Ni+Fe/Al₂O₃-wi (in the range 13 – 63 nm) and CNT@Ni+Fe/Al₂O₃-cp (9 – 33 nm). On the contrary, materials with lower external diameters were obtained when employing the Ni/Al₂O₃-wi and Ni+Fe+Al-cp catalysts, namely in CNT@Ni/Al₂O₃-wi (8 – 32 nm) and CNT@Ni+Fe+Al-cp (4 – 23 nm). Moreover, a wide external diameter distribution range was observed in all the materials. This can be ascribed to the use of thermal decomposition products of LDPE as feedstock for the growth of carbon filaments, since a wide variety of volatile hydrocarbons (*e.g.*, ethene, propene, 1,3-butadiene, methane, 1-butene, n-hexane, isobutene and ethane) are in this way fed to the CVD system (Marcilla et al., 2007).

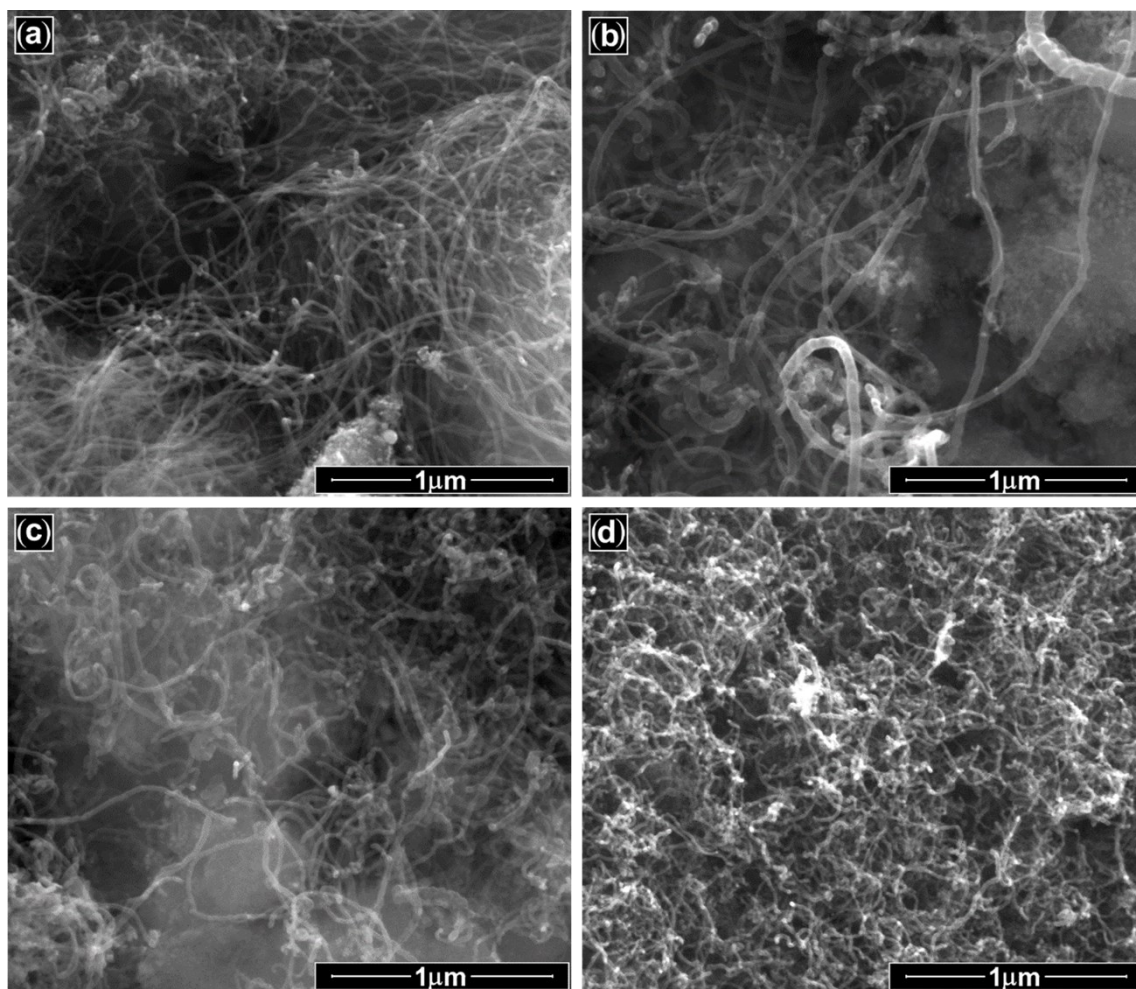


Figure 1. Scanning electron microscopy (SEM) micrographs of the carbon nanotubes (CNTs) obtained by chemical vapour deposition (CVD) over different metal catalysts and using low-density polyethylene (LDPE) as carbon feedstock: (a) CNT@Ni/Al₂O₃-wi, (b) CNT@Ni+Fe/Al₂O₃-wi, (c) CNT@Ni+Fe/Al₂O₃-cp, and (d) CNT@Ni+Fe+Al-cp.

Fibrous carbon materials, such as CNTs and carbon nanofibers (CNFs), are commonly differentiated by the existence/absence of a hollow cavity within their filaments. Unlike CNTs, CNFs do not have (or have very thin) hollow cavities (Serp and Machado, 2015; Tessonier et al., 2009). Bearing this in mind, the morphology of the carbon filaments herein prepared from LDPE was characterized by TEM (*cf.* Figure 2). Hollow cavities are clearly observed in all materials, regardless of the catalyst employed in the CVD system, allowing to conclude that the

proposed methodology is suitable for the synthesis of CNTs. In this case, slightly different internal diameters are observed: CNT@Ni+Fe/Al₂O₃-wi (8 – 14 nm) > CNT@Ni+Fe/Al₂O₃-cp (4 – 12 nm) > CNT@Ni+Fe+Al-cp (2 – 12 nm) > CNT@Ni/Al₂O₃-wi (4 – 10 nm). Regarding the morphology, CNT@Ni/Al₂O₃-wi are similar to standard CNTs (*cf.* Figure 2a), whereas CNT@Ni+Fe/Al₂O₃-wi reveals some cup-stacked tubes (*cf.* Figure 2b), and CNT@Ni+Fe/Al₂O₃-cp and CNT@Ni+Fe+Al-cp (*i.e.*, the materials obtained with metal catalysts prepared by co-precipitation) reveal some helical tubes (*cf.* Figures 2c and d, respectively). Moreover, some metal particles encapsulated within the tubes (not removed upon purification with H₂SO₄ at 140 °C) are observed in all the samples (*cf.* Figure 2). This is a common feature, since encapsulation of catalyst nanoparticles typically occurs during CVD (Menezes et al., 2015). The elemental composition of the nanoparticles trapped within the tubes was qualitatively analysed by EDS (*cf.* Figure S4). As observed, Ni and/or Fe, and Al and O are the main constituents of the observed nanoparticles, confirming that these arise from the metal catalysts employed in the CVD process.

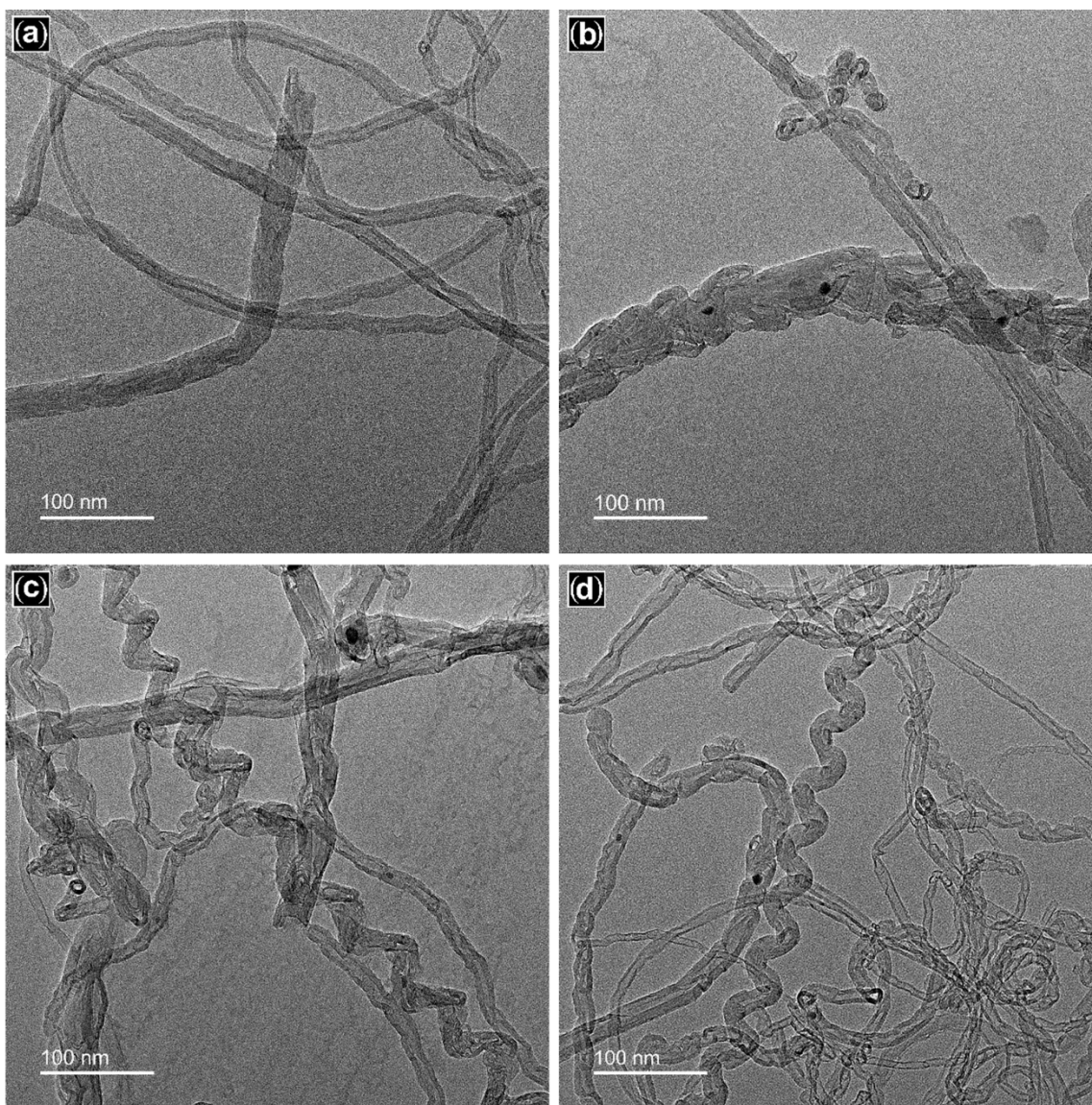


Figure 2. Transmission electron microscopy (TEM) micrographs of the carbon nanotubes (CNTs) obtained by chemical vapour deposition (CVD) over different metal catalysts and using low-density polyethylene (LDPE) as carbon feedstock: (a) CNT@Ni/Al₂O₃-wi, (b) CNT@Ni+Fe/Al₂O₃-wi, (c) CNT@Ni+Fe/Al₂O₃-cp, and (d) CNT@Ni+Fe+Al-cp.

The textural properties of the CNTs (surface area and porosity) were characterized by N₂ physisorption. The adsorption isotherms are shown in Figure S5, and the corresponding results compiled in Table 1. As observed, CNT@Ni/Al₂O₃-wi possesses the highest S_{BET} (226 m² g⁻¹), whereas similar values are obtained for the CNTs prepared from the three catalysts containing

both Ni and Fe (S_{BET} in the range 151 – 155 $\text{m}^2 \text{g}^{-1}$). These values are in line with those commonly determined for CNTs (in the range 10 – 500 $\text{m}^2 \text{g}^{-1}$) (Lehman et al., 2011). Indeed, in a previous work of our group, the S_{BET} of six samples of commercially available CNTs was in the range 41 – 291 $\text{m}^2 \text{g}^{-1}$, and V_{Total} in the range 0.17 – 3.2 $\text{cm}^3 \text{g}^{-1}$ (Pinho et al., 2015). In the case of the CNTs herein produced from LDPE, V_{Total} was in the range 0.657 – 1.042 $\text{cm}^3 \text{g}^{-1}$. The highest value was obtained for CNT@Ni+Fe/Al₂O₃-cp and the lowest for CNT@Ni+Fe+Al-cp.

Table 1. Properties of the carbon nanotubes (CNTs) obtained by chemical vapour deposition (CVD) over different metal catalysts and using low-density polyethylene (LDPE) as carbon feedstock: specific surface area (S_{BET}), total pore volume (V_{Total}), acid-base properties, and pH at the point of zero charge (pH_{PZC})

Material	S_{BET} ($\text{m}^2 \text{g}^{-1}$)	V_{Total} ($\text{cm}^3 \text{g}^{-1}$)	Acidity ($\mu\text{mol L}^{-1}$)	Basicity ($\mu\text{mol L}^{-1}$)	pH_{PZC}
CNT@Ni/Al ₂ O ₃ -wi	226	0.739	85	72	4.0
CNT@Ni+Fe/Al ₂ O ₃ -wi	151	0.860	82	39	3.3
CNT@Ni+Fe/Al ₂ O ₃ -cp	155	1.042	121	21	2.2
CNT@Ni+Fe+Al-cp	153	0.657	141	20	2.3

The acid-base properties and pH at the point of zero charge (pH_{PZC}) of the CNTs were also determined (*cf.* Table 1). As observed, all the materials have acidic nature, which can be explained by the purification step with H₂SO₄. Nevertheless, CNT@Ni+Fe/Al₂O₃-cp and CNT@Ni+Fe+Al-cp (*i.e.*, the materials prepared from the catalysts obtained by co-precipitation of Ni and Fe over Al₂O₃, and by co-precipitation of Ni, Fe and Al, respectively) possess a slightly stronger acidic nature (as indicated by the lower pH_{PZC} values).

3.2. Activated persulfate oxidation in batch mode

The ability of the four powder samples of CNTs prepared from the LDPE feedstock to act

as catalysts for activated persulfate oxidation and degradation of organic MPs was first evaluated through experiments performed in batch mode and employing aqueous solutions of venlafaxine ($250 \mu\text{g L}^{-1}$) as model system. The concentration of venlafaxine obtained as function of time, and the removals obtained after 90 min in adsorption and activated persulfate oxidation experiments are given in Figure S6 and Figure 3, respectively. Non-catalytic oxidation promoted by SPS is also given in Figure 3. In this case, the removal of venlafaxine can be considered negligible, as it amounts to only *ca.* 8% of its initial content.

Regarding adsorption removals, the sample of CNTs revealing the best performance is CNT@Ni/Al₂O₃-wi (*cf.* Figures 3 and S6), which is also the material with the highest S_{BET} among those under study (*cf.* Table 1), and the only one prepared from a catalyst that does not contain Fe. On the contrary, the CNTs prepared from the three catalysts containing both Ni and Fe reveal both similar adsorption capacities (*cf.* Figures 3 and S6) and textural properties (*cf.* Table 1). It is interesting to observe that the removal of venlafaxine undergoes a great increase when SPS is added in the presence of all the CNTs under study (*cf.* Figures 3 and S6). These results allow concluding that the four CNTs prepared from the LDPE feedstock are effective catalysts for activated persulfate oxidation and degradation of venlafaxine. Specifically, removals in the range 88 – 96% are obtained after 90 min of reaction. Nevertheless, the difference of venlafaxine removal due to SPS addition (d_{Removal} , *i.e.*, the increase of pollutant removal obtained in the activated persulfate oxidation experiments compared to that obtained by adsorption) points out a catalyst with apparently higher activity (*cf.* Figure 3). This corresponds to the maximum value of d_{Removal} , obtained when employing CNT@Ni+Fe/Al₂O₃-cp. This enhanced performance for persulfate activation and degradation of venlafaxine becomes even more interesting when the residual metal content of the CNTs samples (*cf.* Table S2) are compared, since CNT@Ni+Fe/Al₂O₃-cp is one of the samples with the lowest content of metal species after the purification step with H₂SO₄ employed at the end of the synthesis

procedure, corresponding to only 0.1 wt.%.

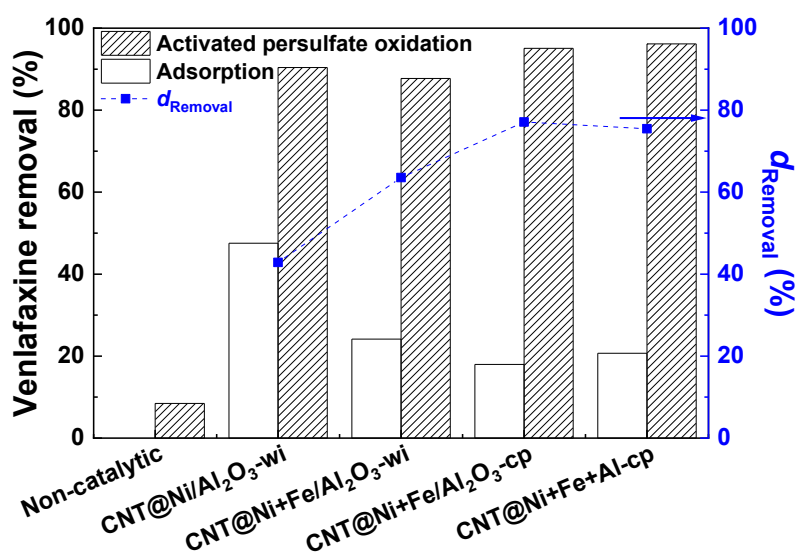


Figure 3. Removal of venlafaxine obtained after 90 min in adsorption and activated persulfate oxidation experiments (bars/left axis) performed in ultrapure (UP) water, and respective difference due to the addition of SPS [d_{Removal} (squares/right axis)]. Experiments performed in batch mode, with $[\text{venlafaxine}]_0 = 250 \mu\text{g L}^{-1}$, $[\text{catalyst/adsorbent}] = 0.05 \text{ g L}^{-1}$, $[\text{SPS}]_0 = 250 \text{ mg L}^{-1}$, $\text{pH}_0 = 5.9$ (inherent pH), and $T = 22 \pm 2 \text{ }^\circ\text{C}$.

The concentration of venlafaxine obtained as function of time in adsorption and activated persulfate oxidation experiments performed with CNT@Ni+Fe/Al₂O₃-cp are detailed in Figure 4, together with the non-catalytic removals promoted by SPS only. In the catalytic experiment, *ca.* 95% of venlafaxine removal is achieved upon 90 min of activated persulfate oxidation, corresponding to a pollutant mass removal rate of $3.17 \text{ mg g}^{-1} \text{ h}^{-1}$ (determined as described in Text S2 and Eq. S1). SPS consumption during this treatment process amounts to 23.7% of its initial content (as determined at the end of the activated persulfate oxidation run). These results confirm the ability of CNT@Ni+Fe/Al₂O₃-cp to activate SPS. Moreover, despite having negligible metal content (*cf.* Table S2), possible metal leaching from CNT@Ni+Fe/Al₂O₃-cp

to the treated water was determined by ICP-OES at the end of the activated persulfate oxidation run. Both Fe and Ni leaching were below 0.05 mg L^{-1} (*i.e.*, the limit of quantification provided by ICP-OES), allowing to conclude about the predominant role of heterogeneous activated persulfate oxidation promoted by CNT@Ni+Fe/Al₂O₃-cp.

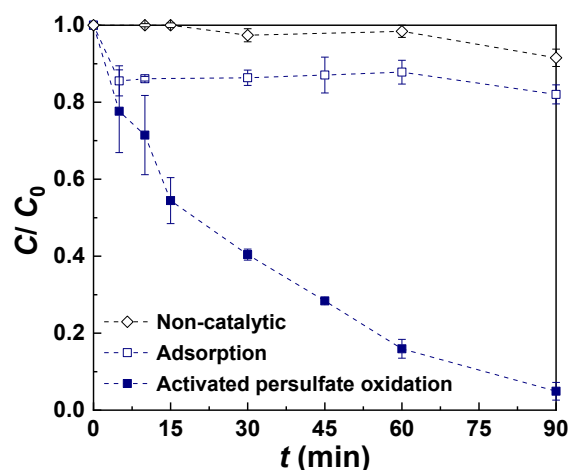


Figure 4. Normalized concentration of venlafaxine obtained as a function of time in adsorption and activated persulfate oxidation experiments performed in ultrapure (UP) water, with CNT@Ni+Fe/Al₂O₃-cp. Non-catalytic removals promoted by SPS are also given. The standard deviation of experimental determination was obtained in experiments performed in duplicate. Experiments performed in batch mode, with $[\text{venlafaxine}]_0 = 250 \text{ } \mu\text{g L}^{-1}$, $[\text{catalyst/adsorbent}] = 0.05 \text{ g L}^{-1}$, $[\text{SPS}]_0 = 250 \text{ mg L}^{-1}$, $\text{pH}_0 = 5.9$ (inherent pH), and $T = 22 \pm 2 \text{ } ^\circ\text{C}$.

The influence of catalyst dosage on the removal of venlafaxine was briefly investigated (*cf.* Figure S7). As observed, venlafaxine is completely removed when the concentration of CNTs is increased to 0.25 g L^{-1} (*cf.* Figure S7b). However, this enhanced pollutant removal can be explained by the higher contribution of the adsorption component. Therefore, a catalyst/adsorbent concentration of 0.05 g L^{-1} was selected for the subsequent studies performed in batch mode, namely regarding the simultaneous removal of four MPs. An aqueous solution containing atenolol, metoprolol and citalopram ($250 \text{ } \mu\text{g L}^{-1}$ of each) was used for that purpose.

As observed (*cf.* Figure S8), CNT@Ni+Fe/Al₂O₃-cp also performed better under these conditions, promoting higher removals of atenolol, venlafaxine and citalopram, and similar removals of metoprolol. Accordingly, the adsorption and activated persulfate oxidation experiments performed with CNT@Ni+Fe/Al₂O₃-cp are detailed in Figures S9a and b, respectively. As observed, the removal of the organic MPs was higher in the activated persulfate oxidation run, but particularly for citalopram and venlafaxine, allowing to conclude that CNT@Ni+Fe/Al₂O₃-cp is an active catalyst for activated persulfate oxidation of these organic MPs. Nevertheless, after *ca.* 15 min of reaction, the concentration of atenolol increased slightly, and was kept above its initial concentration (*i.e.*, $C/C_0 > 1$) for at least 45 min, period after which it decreased again (*cf.* Figure S9b). This is an uncommon observation; thus, although studying the MPs conversion pathway is not a goal of this study, additional investigations were conducted to clarify this trend. Upon carefully analysing the chemical structure of the pollutants under study (*cf.* Table S3), the seemingly most plausible explanation is the conversion of metoprolol into atenolol. Bearing this in mind, an additional activated persulfate oxidation experiment was performed with an aqueous solution containing metoprolol only. As observed, atenolol is indeed formed as metoprolol is degraded under these conditions (*cf.* Figure S10). Since the exact mechanism behind the conversion of metoprolol into atenolol is still unknown, the results herein observed should prompt additional studies on the topic.

The influence of the water matrix on venlafaxine removal by activated persulfate oxidation promoted by CNT@Ni+Fe/Al₂O₃-cp was also studied (*cf.* Figure 5a). For comparison purposes, the removals obtained by adsorption and non-catalytic conversion promoted by SPS are shown in Figure S11. As observed in Figure 5a, the efficiency of the activated persulfate oxidation process increases when the venlafaxine solutions are prepared in DW instead of UP water, whereas employing SW has a negligible effect. Several ions naturally occurring in environmental water matrices (*e.g.*, chloride and bicarbonate ions) are known to affect the

performance of activated persulfate oxidation. On that regard, both beneficial and detrimental effects have been reported (Bennedsen et al., 2012; Fang et al., 2012; Lutze et al., 2015; Matzek and Carter, 2016). Indeed, in a previous work of our group, the reaction rate of bisphenol A degradation by activated persulfate oxidation promoted by a carbon-based catalyst was shown to increase 6-fold when the UP water was added 200 mg L⁻¹ of chloride – an effect ascribed to the formation of chlorine radicals upon reaction of sulphate radicals with chloride ions (Outsiou et al., 2017). The DW employed in the present study is bottled mineral water, which inherently contains chloride ions (5.6 mg L⁻¹). Therefore, the enhanced removal of venlafaxine obtained in DW can be mainly explained by the presence of chloride ions.

Scavenging tests with methanol (MeOH) and furfuryl alcohol (FFA) were then carried out to provide preliminary insights on the main reactive species involved in the activated persulfate oxidation of venlafaxine promoted by CNT@Ni+Fe/Al₂O₃-cp (*cf.* Figure 5b). As observed, venlafaxine removal was slightly suppressed by MeOH, and almost entirely suppressed by FFA. MeOH has strong affinity towards both sulphate (Neta et al., 1996) and hydroxyl (Buxton et al., 1988) radicals, and low affinity towards singlet oxygen (Wilkinson et al., 1995); whereas FFA has strong affinity towards hydroxyl radicals (Buxton et al., 1988) and singlet oxygen (Wilkinson et al., 1995), and most likely also towards sulphate radicals (reaction rate constants not available). Therefore, the results shown in Figure 5b provide a preliminary indication about the predominant role of singlet oxygen in the (non-radical) activated persulfate oxidation of venlafaxine in the presence of CNT@Ni+Fe/Al₂O₃-cp.

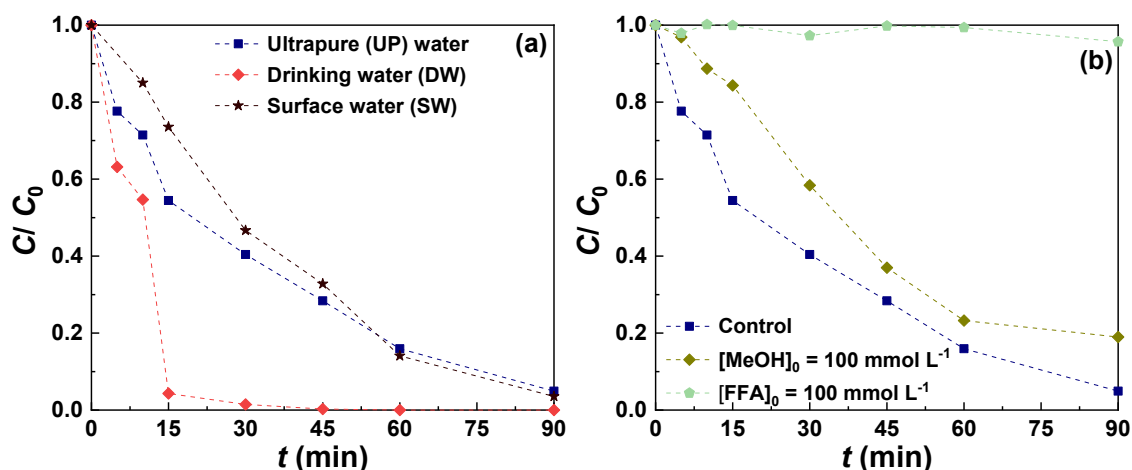


Figure 5. Effect of (a) water matrix, and (b) methanol (MeOH) and furfuryl alcohol (FFA) on the removal of venlafaxine by activated persulfate oxidation in the presence of CNT@Ni+Fe/Al₂O₃-cp. Experiments performed in batch mode, with $[\text{venlafaxine}]_0 = 250 \text{ } \mu\text{g L}^{-1}$, $[\text{CNT@Ni+Fe/Al}_2\text{O}_3\text{-cp}] = 0.05 \text{ g L}^{-1}$, $[\text{SPS}]_0 = 250 \text{ mg L}^{-1}$, $\text{pH}_0 = 5.9, 6.8$ and 7.5 (inherent pH of UP water, DW and SW, respectively), and $T = 22 \pm 2 \text{ } ^\circ\text{C}$.

3.3. Activated persulfate oxidation in continuous mode: a proof of concept

Considering the catalytic activity revealed by CNT@Ni+Fe/Al₂O₃-cp in the activated persulfate oxidation experiments performed in batch mode, additional experiments were performed in continuous mode of operation. For that purpose, a carbon-based catalytic membrane was prepared by including CNT@Ni+Fe/Al₂O₃-cp within a PVDF matrix, through a fabrication methodology previously reported by our group (Vieira et al., 2020), and placed in a glass cell to which a pollutant solution was fed under constant flow conditions (Miller et al., 2014). The experimental setup used to conduct these experiments is depicted in Figure S3. Nor the fabrication methodology (*cf.* Section 2.4 and text S1), nor the operating conditions were optimized, since the goal is to provide an early proof of concept that this material can be applied for the removal of venlafaxine ($100 \text{ } \mu\text{g L}^{-1}$) in continuous mode during a longer period (24 h),

considering the same dosage of SPS as in batch experiments, and employing SW as water matrix. Thus, additional studies may eventually be focused on optimizing this approach.

Adsorption removals were studied first (*cf.* Figure 6a). As observed, the venlafaxine removal reached *ca.* 30% at the beginning of the adsorption experiment, then decreasing as the membrane becomes increasingly saturated. On the contrary, a sharp decrease of the venlafaxine concentration is observed when SPS is added (*cf.* Figure 6b). In this case, venlafaxine removals up to *ca.* 95% are observed within the first 1.5 h of operation in continuous mode, the performance of the process then slightly decreasing and being kept nearly constant (steady state) for the remaining period 5 – 24 h. For instance, venlafaxine removal is still high at the end of the experiment (*ca.* 71% of its initial content), corresponding to a pollutant mass removal rate of $1.97 \text{ mg m}^{-2} \text{ h}^{-1}$ (determined as described in Text S2 and Eq. S3). Moreover, SPS consumption was observed during the entire experiment (*cf.* Figure 6b), allowing to conclude that the composite polymeric membrane can promote the decomposition of SPS. Water permeate flux (J_w ; determined as described in Text S2 and Eq. S2) was also monitored. As observed, J_w is nearly constant during the activated persulfate oxidation experiment (*cf.* Figure 6b), allowing to conclude that membrane fouling is apparently negligible. Taking all into consideration, it can be concluded that the composite polymeric membrane is effective for activated persulfate oxidation in continuous mode of operation and degradation of venlafaxine in SW.

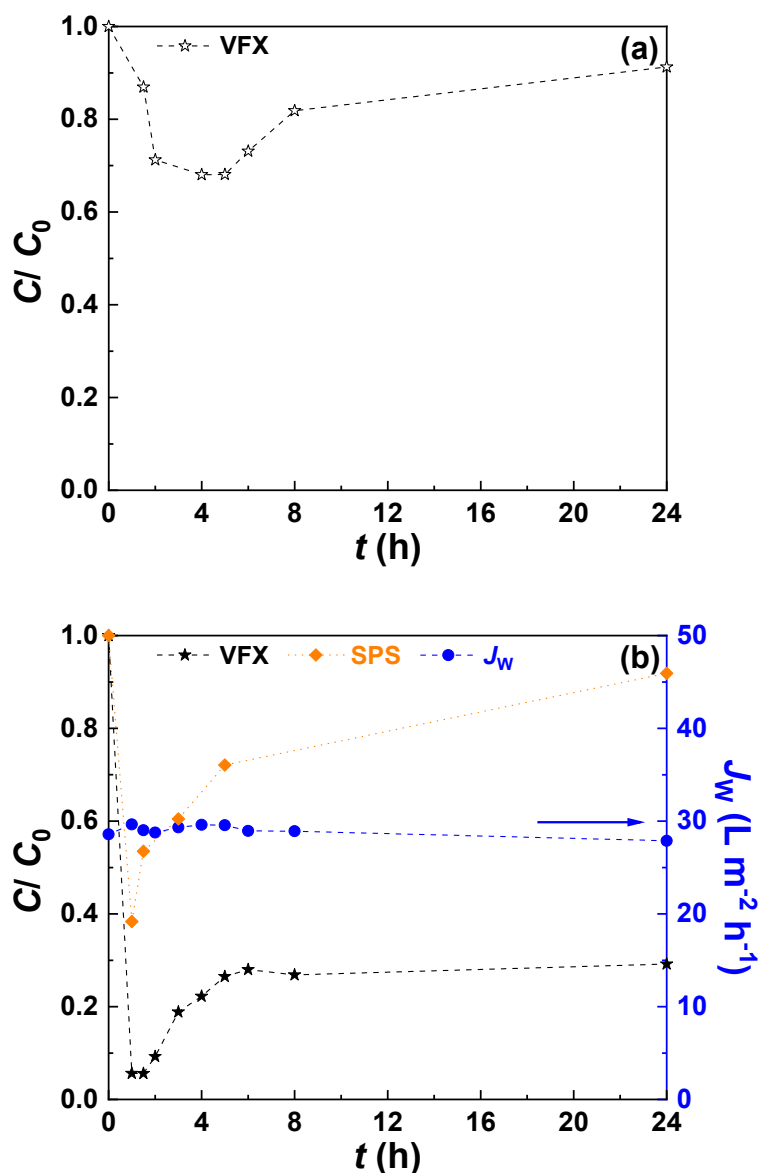


Figure 6. Normalized concentration of venlafaxine obtained as function of time in (a) adsorption and (b) activated persulfate oxidation experiments performed in surface water (SW), with composite CNT@Ni+Fe/Al₂O₃-cp-PVDF membranes. Water permeate flux (J_w) and conversion of SPS are also shown in (b). Experiments performed in continuous mode, with $[venlafaxine]_0 = 100 \mu g L^{-1}$, $[SPS]_0 = 250 mg L^{-1}$, $pH_0 = 7.5$ (inherent pH), $Q = 0.1 mL min^{-1}$, and $T = 22 \pm 2 \text{ } ^\circ C$.

Conclusions

Low-density polyethylene (LDPE) was a suitable carbon feedstock for the growth of carbon nanotubes (CNTs) by chemical vapour deposition (CVD) using four different metal-based catalysts (Al_2O_3 , Ni, Fe and/or Al). For the first time, LDPE derived CNTs were demonstrated to be active catalysts for persulfate activation and degradation of organic micropollutants. The best performing CNTs in batch mode of operation (CNT@Ni+Fe/ Al_2O_3 -cp) were also active for the removal of venlafaxine as model compound in relevant environmental water matrices, such as surface water. These CNTs were used to fabricate a composite polymeric membrane with poly(vinylidene fluoride) - PVDF that was effective for venlafaxine removal in continuous mode of operation using surface water.

Acknowledgments

This work was financially supported by project POCI-01-0145-FEDER-031439 (PLASTIC TO FUEL&MAT) funded by FEDER funds through COMPETE2020 – Programa Operacional Competitividade e Internacionalização (POCI), and by national funds (PIDDAC) through FCT/MCTES. We would also like to thank the scientific collaboration under Base-UIDB/50020/2020 and Programmatic-UIDP/50020/2020 Funding of LSRE-LCM - funded by national funds through FCT/MCTES (PIDDAC), Base Funding UIDB/00690/2020 of the Centro de Investigação de Montanha (CIMO) - funded by national funds through FCT/MCTES (PIDDAC), and projects NORTE-01-0145-FEDER-031049 (InSpeCt - PTDC/EAM-AMB/31049/2017) funded by FEDER funds through NORTE 2020 - Programa Operacional Regional do NORTE, and by national funds (PIDDAC) through FCT/MCTES, and NORTE-01-0145-FEDER-000069 (*Healthy Waters*) funded by NORTE 2020 under the PORTUGAL 2020 Partnership Agreement through FEDER. Fernanda Fontana Roman also thanks to the FCT

for the individual research grant SFRH/BD/143224/2019. Technical assistance with SEM analysis is gratefully acknowledged to CEMUP team.

References

Barbosa, M.O., Lado Ribeiro, A.R., Ratola, N., Hain, E., Homem, V., Pereira, M.F.R., Blaney, L., Silva, A.M.T., 2018. Spatial and seasonal occurrence of micropollutants in four Portuguese rivers and a case study for fluorescence excitation-emission matrices. *Sci. Total Environ.* 644, 1128-1140. <https://doi.org/10.1016/j.scitotenv.2018.06.355>

Bazargan, A., McKay, G., 2012. A review – Synthesis of carbon nanotubes from plastic wastes. *Chem. Eng. J.* 195-196, 377-391. <https://doi.org/10.1016/j.cej.2012.03.077>

Bennedsen, L.R., Muff, J., Søgaaard, E.G., 2012. Influence of chloride and carbonates on the reactivity of activated persulfate. *Chemosphere* 86, 1092-1097. <https://doi.org/10.1016/j.chemosphere.2011.12.011>

Borsodi, N., Szentes, A., Miskolczi, N., Wu, C., Liu, X., 2016. Carbon nanotubes synthesized from gaseous products of waste polymer pyrolysis and their application. *J. Anal. Appl. Pyrolysis* 120, 304-313. <https://doi.org/10.1016/j.jaap.2016.05.018>

Buxton, G.V., Greenstock, C.L., Helman, W.P., Ross, A.B., 1988. Critical Review of rate constants for reactions of hydrated electrons, hydrogen atoms and hydroxyl radicals (HO[•]/O^{•-}) in aqueous solution. *J. Phys. Chem. Ref. Data* 17, 513-886. <https://doi.org/10.1063/1.555805>

Cai, N., Xia, S., Zhang, X., Meng, Z., Bartocci, P., Fantozzi, F., Chen, Y., Chen, H., Williams, P.T., Yang, H., 2020a. Preparation of iron- and nitrogen-codoped carbon nanotubes from waste plastics pyrolysis for the oxygen reduction reaction. *ChemSusChem* 13, 938-944. <https://doi.org/10.1002/cssc.201903293>

Cai, N., Yang, H., Zhang, X., Xia, S., Yao, D., Bartocci, P., Fantozzi, F., Chen, Y., Chen, H., Williams, P.T., 2020b. Bimetallic carbon nanotube encapsulated Fe-Ni catalysts from fast

pyrolysis of waste plastics and their oxygen reduction properties. *Waste Manage.* 109, 119-126.

<https://doi.org/10.1016/j.wasman.2020.05.003>

Chen, X., Oh, W.-D., Lim, T.-T., 2018. Graphene- and CNTs-based carbocatalysts in persulfates activation: Material design and catalytic mechanisms. *Chem. Eng. J.* 354, 941-976.

<https://doi.org/10.1016/j.cej.2018.08.049>

Deokar, S.K., Bajad, G.S., Bhonde, P., Vijayakumar, R.P., Mandavgane, S.A., 2017. Adsorptive removal of diuron herbicide on carbon nanotubes synthesized from plastic waste. *J. Polym. Environ.* 25, 165-175.

<https://doi.org/10.1007/s10924-016-0794-3>

Duan, X., Sun, H., Wang, S., 2018. Metal-free carbocatalysis in advanced oxidation reactions.

Acc. Chem. Res. 51, 678-687. <https://doi.org/10.1021/acs.accounts.7b00535>

EU Commission, 2020. Commission Implementing Decision (EU) 2020/1161 of 4 August 2020 establishing a watch list of substances for Union-wide monitoring in the field of water policy pursuant to Directive 2008/105/EC of the European Parliament and of the Council. *Official Journal of the European Union.* https://eur-lex.europa.eu/eli/dec_impl/2020/1161/oj

Fang, G.-D., Dionysiou, D.D., Wang, Y., Al-Abed, S.R., Zhou, D.-M., 2012. Sulfate radical-based degradation of polychlorinated biphenyls: Effects of chloride ion and reaction kinetics.

J. Hazard. Mater. 227-228, 394-401. <https://doi.org/10.1016/j.jhazmat.2012.05.074>

Gao, L., Zhou, F., Chen, Q., Duan, G., 2018. Generation of Pd@Ni-CNTs from polyethylene wastes and their application in the electrochemical hydrogen evolution reaction.

ChemistrySelect 3, 5321-5325. <https://doi.org/10.1002/slct.201800127>

Gomes, H.T., Miranda, S.M., Sampaio, M.J., Silva, A.M.T., Faria, J.L., 2010. Activated carbons treated with sulphuric acid: catalysts for catalytic wet peroxide oxidation. *Catal. Today* 151, 153-158. <https://doi.org/10.1016/j.cattod.2010.01.017>

Gong, J., Liu, J., Chen, X., Jiang, Z., Wen, X., Mijowska, E., Tang, T., 2014. Striking influence of NiO catalyst diameter on the carbonization of polypropylene into carbon nanomaterials and

their high performance in the adsorption of oils. *RSC Adv.* 4, 33806-33814.

<https://doi.org/10.1039/C4RA05016A>

Lehman, J.H., Terrones, M., Mansfield, E., Hurst, K.E., Meunier, V., 2011. Evaluating the characteristics of multiwall carbon nanotubes. *Carbon* 49, 2581-2602.

<https://doi.org/10.1016/j.carbon.2011.03.028>

Lutze, H.V., Kerlin, N., Schmidt, T.C., 2015. Sulfate radical-based water treatment in presence of chloride: Formation of chlorate, inter-conversion of sulfate radicals into hydroxyl radicals and influence of bicarbonate. *Water Res.* 72, 349-360.

<https://doi.org/10.1016/j.watres.2014.10.006>

Marcilla, A., García, Á.N., del Remedio Hernández, M., 2007. Thermal degradation of LDPE–vacuum gas oil mixtures for plastic wastes valorization. *Energ. Fuel.* 21, 870-880.

<https://doi.org/10.1021/ef0605293>

Matzek, L.W., Carter, K.E., 2016. Activated persulfate for organic chemical degradation: a review. *Chemosphere* 151, 178-188. <http://dx.doi.org/10.1016/j.chemosphere.2016.02.055>

Menezes, H.C., de Barcelos, S.M.R., Macedo, D.F.D., Purceno, A.D., Machado, B.F., Teixeira, A.P.C., Lago, R.M., Serp, P., Cardeal, Z.L., 2015. Magnetic N-doped carbon nanotubes: A versatile and efficient material for the determination of polycyclic aromatic hydrocarbons in environmental water samples. *Anal. Chim. Acta* 873, 51-56.

<https://doi.org/10.1016/j.aca.2015.02.063>

Mezni, A., Saber, N.B., Alhadhrami, A.A., Gobouri, A., Aldalbahi, A., Hay, S., Santos, A., Losic, D., Altalhi, T., 2017. Highly biocompatible carbon nanocapsules derived from plastic waste for advanced cancer therapy. *J. Drug Deliv. Sci. Technol.* 41, 351-358.

<https://doi.org/10.1016/j.jddst.2017.08.007>

Miller, D.J., Kasemset, S., Paul, D.R., Freeman, B.D., 2014. Comparison of membrane fouling at constant flux and constant transmembrane pressure conditions. *J. Membr. Sci.* 454, 505-515. <https://doi.org/10.1016/j.memsci.2013.12.027>

Miranda, M.N., Silva, A.M.T., Pereira, M.F.R., 2020. Microplastics in the environment: A DPSIR analysis with focus on the responses. *Science of the Total Environment* 718. <https://doi.org/10.1016/j.scitotenv.2019.134968>

Moo, J.G.S., Veksha, A., Oh, W.-D., Giannis, A., Udayanga, W.D.C., Lin, S.-X., Ge, L., Lisak, G., 2019. Plastic derived carbon nanotubes for electrocatalytic oxygen reduction reaction: Effects of plastic feedstock and synthesis temperature. *Electrochem. Commun.* 101, 11-18. <https://doi.org/10.1016/j.elecom.2019.02.014>

Neta, P., Grodkowski, J., Ross, A.B., 1996. Rate constants for reactions of aliphatic carbon-centered radicals in aqueous solution. *J. Phys. Chem. Ref. Data* 25, 709-1050. <https://doi.org/10.1063/1.555978>

NIST, 2018. National Institute of Standards and Technology (NIST), NIST Standard Reference Database 69: NIST Chemistry WebBook. U.S. Secretary of Commerce on behalf of the United States of America. <https://doi.org/10.18434/T4D303>

Nyakuma, B.B., Ivase, T.J.-P., Emerging trends in sustainable treatment and valorisation technologies for plastic wastes in Nigeria: A concise review. *Environ. Prog. Sustainable Energy*, e13660. <https://doi.org/10.1002/ep.13660>

Oberlin, A., Endo, M., Koyama, T., 1976. Filamentous growth of carbon through benzene decomposition. *J. Cryst. Growth* 32, 335-349. [https://doi.org/10.1016/0022-0248\(76\)90115-9](https://doi.org/10.1016/0022-0248(76)90115-9)

Okan, M., Aydin, H.M., Barsbay, M., 2019. Current approaches to waste polymer utilization and minimization: A review. *J. Chem. Technol. Biotechnol.* 94, 8-21. <https://doi.org/10.1002/jctb.5778>

Outsiou, A., Frontistis, Z., Ribeiro, R.S., Antonopoulou, M., Konstantinou, I.K., Silva, A.M.T., Faria, J.L., Gomes, H.T., Mantzavinos, D., 2017. Activation of sodium persulfate by magnetic carbon xerogels (CX/CoFe) for the oxidation of bisphenol A: process variables effects, matrix effects and reaction pathways. *Water Res.* 124, 97-107. <https://doi.org/10.1016/j.watres.2017.07.046>

Papari, S., Bamdad, H., Berruti, F., 2021. Pyrolytic conversion of plastic waste to value-added products and fuels: A review. *Materials* 14, 2586. <https://doi.org/10.3390/ma14102586>

Pinho, M.T., Gomes, H.T., Ribeiro, R.S., Faria, J.L., Silva, A.M.T., 2015. Carbon nanotubes as catalysts for catalytic wet peroxide oxidation of highly concentrated phenol solutions: towards process intensification. *Appl. Catal. B* 165, 706-714. <https://doi.org/10.1016/j.apcatb.2014.10.057>

Pol, V.G., Thackeray, M.M., 2011. Spherical carbon particles and carbon nanotubes prepared by autogenic reactions: Evaluation as anodes in lithium electrochemical cells. *Energy Environ. Sci.* 4, 1904-1912. <https://doi.org/10.1039/C0EE00256A>

Ribeiro, R.S., Frontistis, Z., Mantzavinos, D., Venieri, D., Antonopoulou, M., Konstantinou, I., Silva, A.M.T., Faria, J.L., Gomes, H.T., 2016a. Magnetic carbon xerogels for the catalytic wet peroxide oxidation of sulfamethoxazole in environmentally relevant water matrices. *Appl. Catal. B* 199, 170-186. <https://doi.org/10.1016/j.apcatb.2016.06.021>

Ribeiro, R.S., Silva, A.M.T., Figueiredo, J.L., Faria, J.L., Gomes, H.T., 2016b. Catalytic wet peroxide oxidation: a route towards the application of hybrid magnetic carbon nanocomposites for the degradation of organic pollutants. A review. *Appl. Catal. B* 187, 428-460. <https://doi.org/10.1016/j.apcatb.2016.01.033>

Serp, P., Corrias, M., Kalck, P., 2003. Carbon nanotubes and nanofibers in catalysis. *Appl. Catal. A* 253, 337-358. [https://doi.org/10.1016/S0926-860X\(03\)00549-0](https://doi.org/10.1016/S0926-860X(03)00549-0)

Serp, P., Machado, B.F., 2015. Nanostructured carbon materials for catalysis. The Royal Society of Chemistry, Cambridge, UK.

Sharma, S.S., Batra, V.S., 2020. Production of hydrogen and carbon nanotubes via catalytic thermo-chemical conversion of plastic waste: Review. *J. Chem. Technol. Biotechnol.* 95, 11-19. <https://doi.org/10.1002/jctb.6193>

Silva, A.S., Kalmakhanova, M.S., Massalimova, B.K., Sgorlon, J.G., Diaz de Tuesta, J.L., Gomes, H.T., 2019. Wet peroxide oxidation of paracetamol using acid activated and Fe/Co-pillared clay catalysts prepared from natural clays. *Catalysts* 9, 705. <https://doi.org/10.3390/catal9090705>

Sousa, J.C.G., Barbosa, M.O., Lado Ribeiro, A.R., Ratola, N., Pereira, M.F.R., Silva, A.M.T., 2020. Distribution of micropollutants in estuarine and sea water along the Portuguese coast. *Mar. Pollut. Bull.* 154, 111120. <https://doi.org/10.1016/j.marpolbul.2020.111120>

Sridhar, V., Park, H., 2020. Transforming waste poly(ethylene terephthalate) into nitrogen doped carbon nanotubes and Its utility in oxygen reduction reaction and bisphenol-A removal from contaminated water. *Materials* 13, 4144. <https://doi.org/10.3390/ma13184144>

Szabó, A., Perri, C., Csató, A., Giordano, G., Vuono, D., Nagy, J.B., 2010. Synthesis methods of carbon nanotubes and related materials. *Materials* 3, 3092-3140. <https://doi.org/10.3390/ma3053092>

Tessonier, J.-P., Rosenthal, D., Hansen, T.W., Hess, C., Schuster, M.E., Blume, R., Girgsdies, F., Pfänder, N., Timpe, O., Su, D.S., Schlögl, R., 2009. Analysis of the structure and chemical properties of some commercial carbon nanostructures. *Carbon* 47, 1779-1798. <https://doi.org/10.1016/j.carbon.2009.02.032>

Utetiwabo, W., Yang, L., Tufail, M.K., Zhou, L., Chen, R., Lian, Y., Yang, W., 2020. Electrode materials derived from plastic wastes and other industrial wastes for supercapacitors. *Chin. Chem. Lett.* 31, 1474-1489. <https://doi.org/10.1016/j.cclet.2020.01.003>

Veksha, A., Yin, K., Moo, J.G.S., Oh, W.-D., Ahamed, A., Chen, W.Q., Weerachanchai, P., Giannis, A., Lisak, G., 2020. Processing of flexible plastic packaging waste into pyrolysis oil and multi-walled carbon nanotubes for electrocatalytic oxygen reduction. *J. Hazard. Mater.* 387, 121256. <https://doi.org/10.1016/j.jhazmat.2019.121256>

Vieira, O., Ribeiro, R.S., Pedrosa, M., Lado Ribeiro, A.R., Silva, A.M.T., 2020. Nitrogen-doped reduced graphene oxide – PVDF nanocomposite membrane for persulfate activation and degradation of water organic micropollutants. *Chem. Eng. J.* 402, 126117. <https://doi.org/10.1016/j.cej.2020.126117>

Wang, J., Shen, B., Lan, M., Kang, D., Wu, C., 2020. Carbon nanotubes (CNTs) production from catalytic pyrolysis of waste plastics: The influence of catalyst and reaction pressure. *Catal. Today* 351, 50-57. <https://doi.org/10.1016/j.cattod.2019.01.058>

Wen, X., Chen, X., Tian, N., Gong, J., Liu, J., Rummeli, M.H., Chu, P.K., Mijiwska, E., Tang, T., 2014. Nanosized carbon black combined with Ni₂O₃ as “universal” catalysts for synergistically catalyzing carbonization of polyolefin wastes to synthesize carbon nanotubes and application for supercapacitors. *Environ. Sci. Technol.* 48, 4048-4055. <https://doi.org/10.1021/es404646e>

Wilkinson, F., Helman, W.P., Ross, A.B., 1995. Rate constants for the decay and reactions of the lowest electronically excited singlet state of molecular oxygen in solution. An expanded and revised compilation. *J. Phys. Chem. Ref. Data* 24, 663-677. <https://doi.org/10.1063/1.555965>

Williams, P.T., 2021. Hydrogen and carbon nanotubes from pyrolysis-catalysis of waste plastics: A review. *Waste Biomass Valorization* 12, 1-28. <https://doi.org/10.1007/s12649-020-01054-w>

Wu, C., Nahil, M.A., Miskolczi, N., Huang, J., Williams, P.T., 2016. Production and application of carbon nanotubes, as a co-product of hydrogen from the pyrolysis-catalytic reforming of waste plastic. *Process Saf. Environ.* 103, 107-114. <https://doi.org/10.1016/j.psep.2016.07.001>

Zhao, X., Ma, J., Wang, Z., Wen, G., Jiang, J., Shi, F., Sheng, L., 2012. Hyperbranched-polymer functionalized multi-walled carbon nanotubes for poly (vinylidene fluoride) membranes: From dispersion to blended fouling-control membrane. *Desalination* 303, 29-38. <https://doi.org/10.1016/j.desal.2012.07.009>

Zhuo, C., Levendis, Y.A., 2014. Upcycling waste plastics into carbon nanomaterials: A review. *J. Appl. Polym. Sci.* 131. <https://doi.org/10.1002/app.39931>

Supplementary material

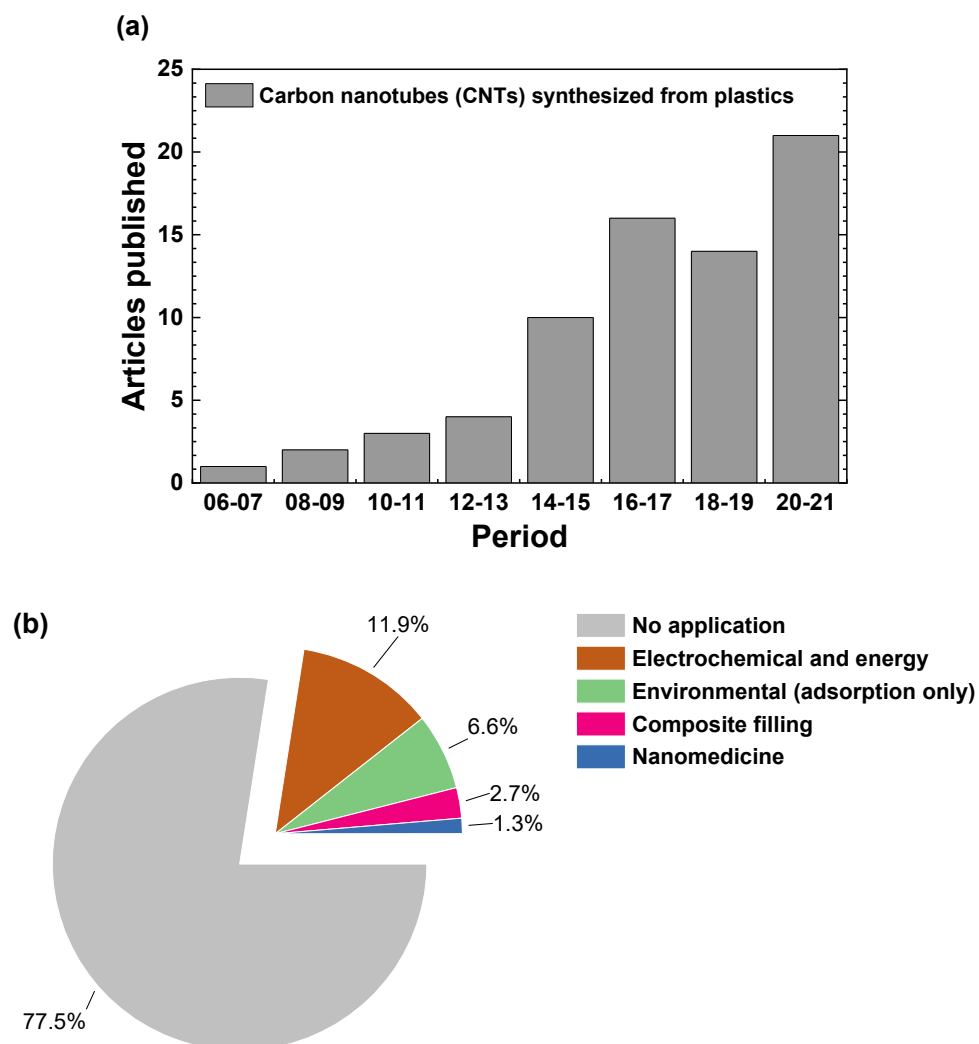


Figure S1. (a) Evolution of the Scopus's indexed original research articles dealing with conversion of plastics into carbon nanotubes (CNTs). (b) Field of application of the CNTs produced from plastics. Data collected from Scopus database on June 29, 2021, using the following search string: “carbon AND nanotube AND plastic AND waste”.

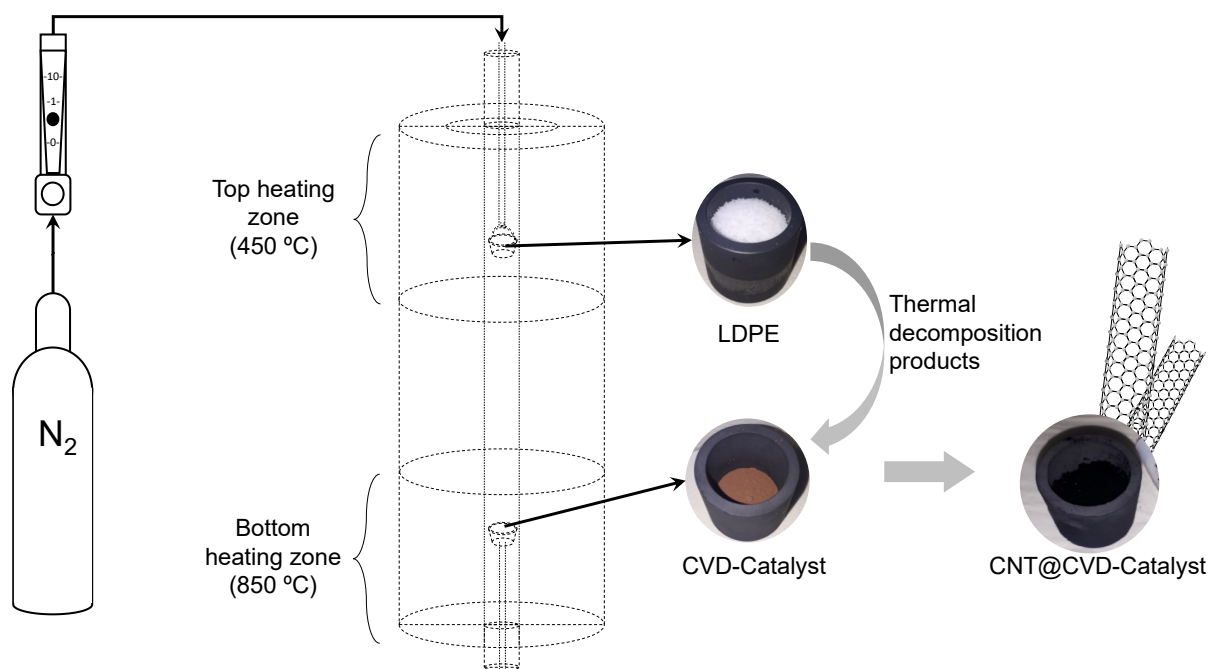


Figure S2. Experimental setup used for the synthesis of CNTs by sequential thermal decomposition of low-density polyethylene (LDPE) and catalytic chemical vapour deposition (CVD) over the prepared catalysts.

Text S1. Detailed description of the procedure used for the fabrication of the CNT@Ni+Fe/Al₂O₃-cp-PVDF composite membranes

Composite CNT@Ni+Fe/Al₂O₃-cp-PVDF membranes were fabricated considering 3.2 wt.% of CNT@Ni+Fe/Al₂O₃-cp in the membrane-forming materials, by adapting the procedure previously reported by our group (Vieira et al., 2020). Accordingly, 0.070 g of polyvinylpyrrolidone (PVP) was dissolved in 6.0 mL of 1-methyl-2-pyrrolidone (NMP), and 0.928 g of powder CNT@Ni+Fe/Al₂O₃-cp added to the resulting solution. After sonication for 3 h at room temperature, 1.07 g of poly(vinylidene fluoride) (PVDF) was added, and the polymerization allowed to proceed in a stirred glass flask kept at 40 °C for 48 h. The resulting polymer solution was left unstirred overnight at room temperature, and then spread in a glass plate with a casting knife film applicator (Elcometer 3580, Warren) set to a thickness of 50 μm. Afterwards, the spread solution was immersed in distilled water for coagulation, the resulting sheet of composite CNT@Ni+Fe/Al₂O₃-cp-PVDF membrane being cut into pieces with 1.64

cm of inner diameter and 2.10 cm² of effective area, which were stored in distilled water until being used.

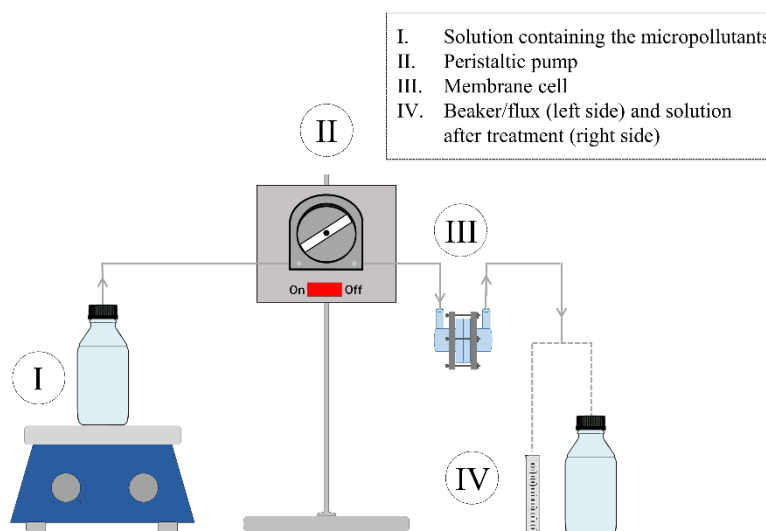


Figure S3. Schematic representation of the experimental setup used for the experiments performed in continuous mode of operation. Reproduced from (Vieira et al., 2020) with permission from Elsevier.

Table S1. Retention time, range, coefficient of determination, method detection limit (DL), and accuracy and inter-batch precision obtained for the organic micropollutants under study, in low, medium, and high concentration levels over the linear range

Compound	Retention time (min)	Range ($\mu\text{g L}^{-1}$)	r^2	DL ($\mu\text{g L}^{-1}$)	Accuracy (%)			Inter-batch precision RSD (%)		
					Low	Medium	High	Low	Medium	High
Atenolol	1.5	2.5 – 300	0.9998	0.7	109.7	101.0	99.5	0.5	1.6	1.8
Metoprolol	2.0	2.5 – 300	0.9998	0.1	103.8	102.0	99.7	0.5	0.2	0.8
Venlafaxine	3.0	2.5 – 300	0.998	0.1	93.9	96.1	102.5	3.1	1.8	1.7
Citalopram	7.0	2.5 - 250	0.998	0.2	102.5	95.1	104.5	4.5	0.6	2.0

Table S2. Metal content of the carbon nanotubes (CNTs) obtained by chemical vapour deposition (CVD) over different metal catalysts and using low-density polyethylene (LDPE) as carbon feedstock, after purification with H₂SO₄. Values obtained by inductively coupled plasma optical emission spectrometry (ICP-OES) analysis of the solution resulting from the acidic digestion of the solids

Material	Metal content (wt.%)			
	Al	Fe	Ni	Total
CNT@Ni/Al ₂ O ₃ -wi	0.32	-	0.92	1.24
CNT@Ni+Fe/Al ₂ O ₃ -wi	0.05	0.04	0.01	0.10
CNT@Ni+Fe/Al ₂ O ₃ -cp	0.02	0.06	0.02	0.10
CNT@Ni+Fe+Al-cp	0.04	0.08	0.03	0.15

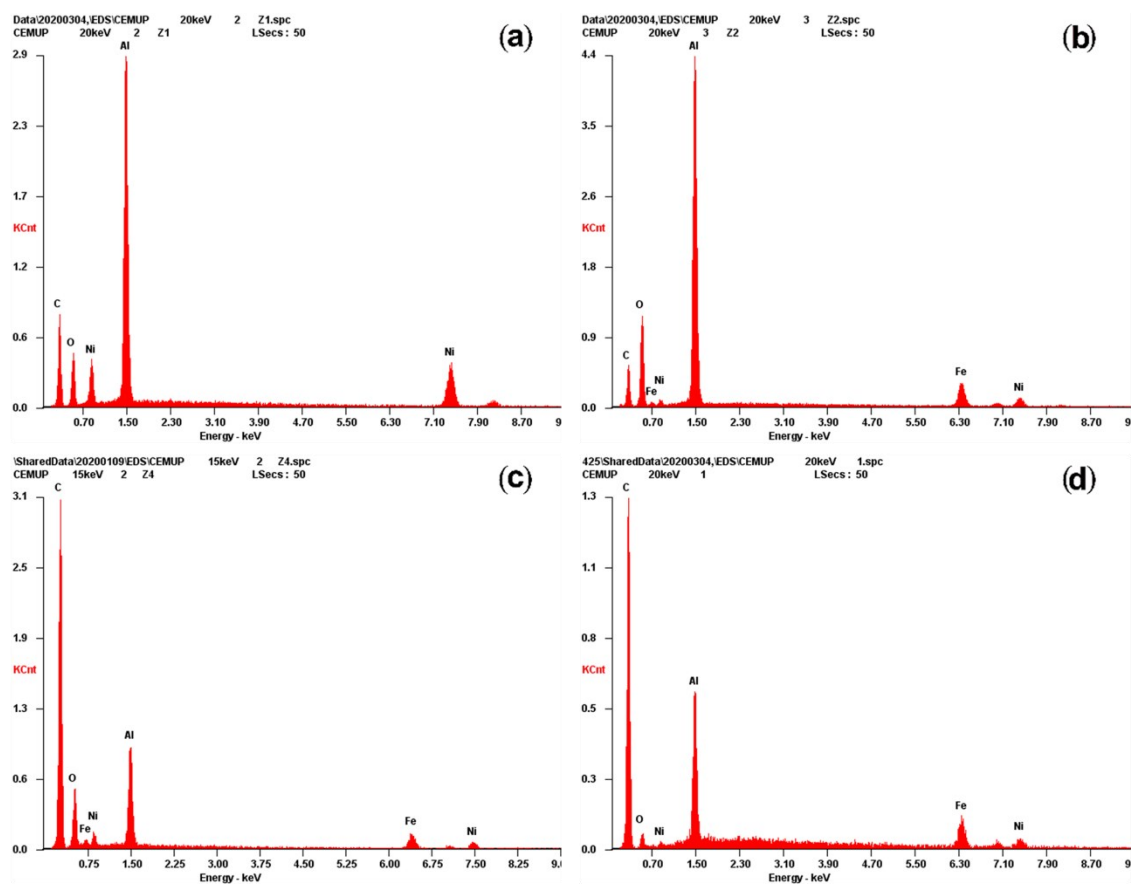


Figure S4. Energy dispersive spectroscopy (EDS) spectra obtained with the electron beam directed onto the centre of particles observed within the carbon nanotubes (CNTs) obtained by chemical vapour deposition (CVD) over different metal catalysts and using low-density polyethylene (LDPE) as carbon feedstock: (a) CNT@Ni/Al₂O₃-wi, (b) CNT@Ni+Fe/Al₂O₃-wi, (c) CNT@Ni+Fe/Al₂O₃-cp, and (d) CNT@Ni+Fe+Al-cp.

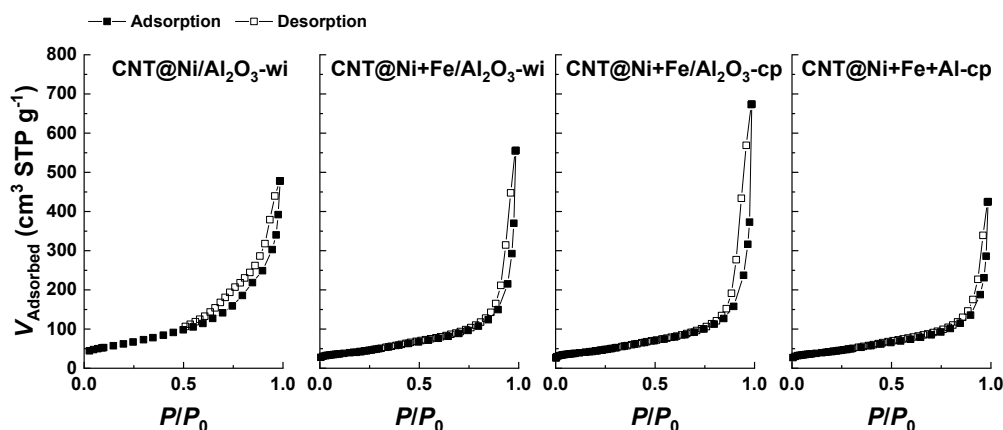


Figure S5. N₂ adsorption-desorption isotherms at -196 °C of the carbon nanotubes (CNTs) obtained by chemical vapour deposition (CVD) over different metal catalysts and using low-density polyethylene (LDPE) as carbon feedstock.

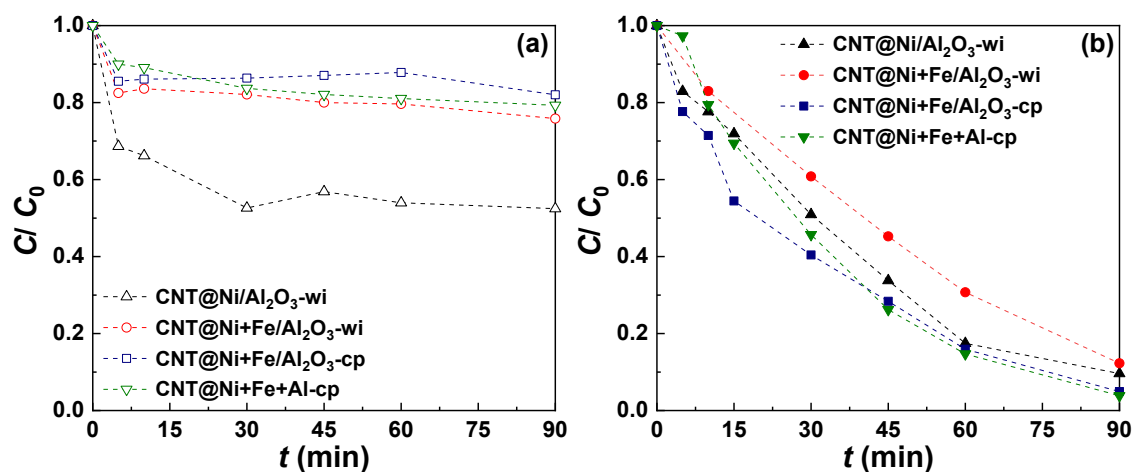


Figure S6. Normalized concentration of venlafaxine obtained as function of time in (a) adsorption and (b) activated persulfate oxidation experiments performed in ultrapure (UP) water, with different CNTs. Experiments performed in batch mode, with $[\text{venlafaxine}]_0 = 250 \mu\text{g L}^{-1}$, $[\text{catalyst/adsorbent}] = 0.05 \text{ g L}^{-1}$, $[\text{SPS}]_0 = 250 \text{ mg L}^{-1}$, $\text{pH}_0 = 5.9$ (inherent pH), and $T = 22 \pm 2 \text{ }^\circ\text{C}$.

Text S2. Performance evaluation

Experiments in batch mode

The performance of powder CNT@Ni+Fe/Al₂O₃-cp for activation of SPS and degradation of venlafaxine was evaluated through an additional parameter, defined as pollutant mass removal rate in batch mode ($m_{\text{Removal, batch}}$), and obtained as described in Eq. S1. [Venlafaxine]₀ and [Venlafaxine]_t represent the concentration of venlafaxine at the beginning of the experiment and at a given time t , respectively.

$$m_{\text{Removal, batch}} = \frac{[\text{Venlafaxine}]_0 - [\text{Venlafaxine}]_t}{\frac{[\text{CNT@Ni+FeAl}_2\text{O}_3\text{-cp}]}{t}} \quad (\text{S1})$$

Experiments in continuous mode

Water permeate flux (J_w) in experiments performed in continuous mode of operation was calculated as described in Eq. S2, in which V , S and Δt represent the volume of permeated water, effective area of the membrane, and permeation time, respectively (Zhao et al., 2012). The performance of the composite polymeric membrane for SPS activation and degradation of venlafaxine was evaluated through an additional parameter, defined as pollutant mass removal rate in continuous mode ($m_{\text{Removal, continuous}}$), and obtained as described in Eq. S3. [Venlafaxine]₀ and [Venlafaxine]_{Effluent} represent the concentration of venlafaxine in the influent and effluent of the membrane cell, respectively.

$$J_w = \frac{V}{S \Delta t} \quad (\text{S2})$$

$$m_{\text{Removal, continuous}} = J_w \times ([\text{Venlafaxine}]_0 - [\text{Venlafaxine}]_{\text{Effluent}}) \quad (\text{S3})$$

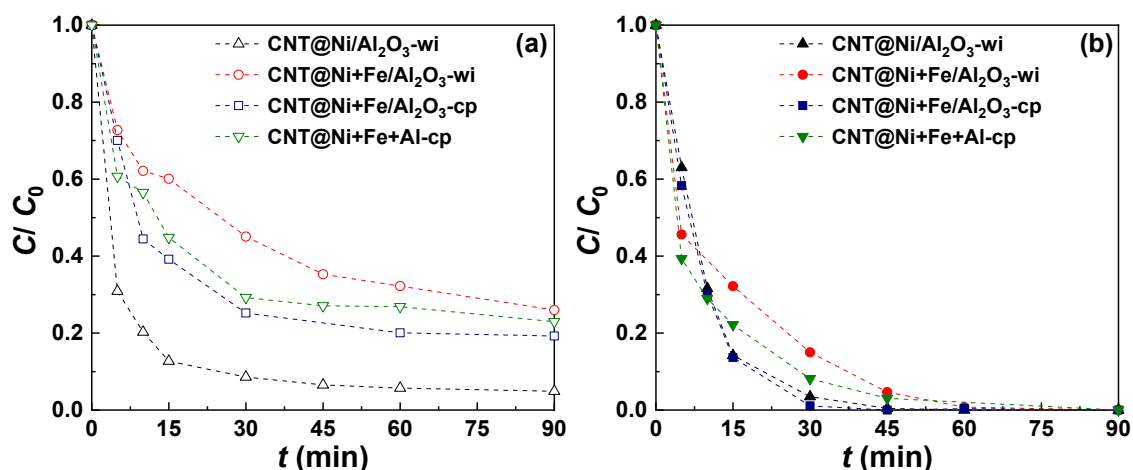


Figure S7. Normalized concentration of venlafaxine obtained as function of time in (a) adsorption and (b) activated persulfate oxidation experiments performed in ultrapure (UP) water, with different CNTs. Experiments performed in batch mode, with $[\text{venlafaxine}]_0 = 250 \mu\text{g L}^{-1}$, $[\text{catalyst/adsorbent}] = 0.25 \text{ g L}^{-1}$, $[\text{SPS}]_0 = 250 \text{ mg L}^{-1}$, $\text{pH}_0 = 5.9$ (inherent pH), and $T = 22 \pm 2 \text{ }^\circ\text{C}$.

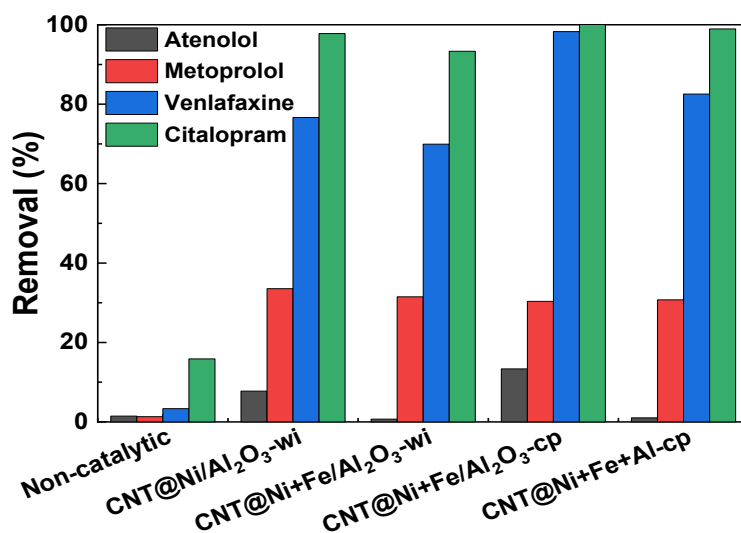


Figure S8. Removal of atenolol, metoprolol, venlafaxine, and citalopram obtained after 90 min in adsorption and activated persulfate oxidation experiments (bars/left axis) performed in ultrapure (UP) water. Experiments performed in batch mode, with $[\text{atenolol}]_0 = [\text{metoprolol}]_0 = [\text{venlafaxine}]_0 = [\text{citalopram}]_0 = 250 \mu\text{g L}^{-1}$, $[\text{catalyst}] = 0.05 \text{ g L}^{-1}$, $[\text{SPS}]_0 = 250 \text{ mg L}^{-1}$, $\text{pH}_0 = 5.9$ (inherent pH), and $T = 22 \pm 2 \text{ }^\circ\text{C}$.

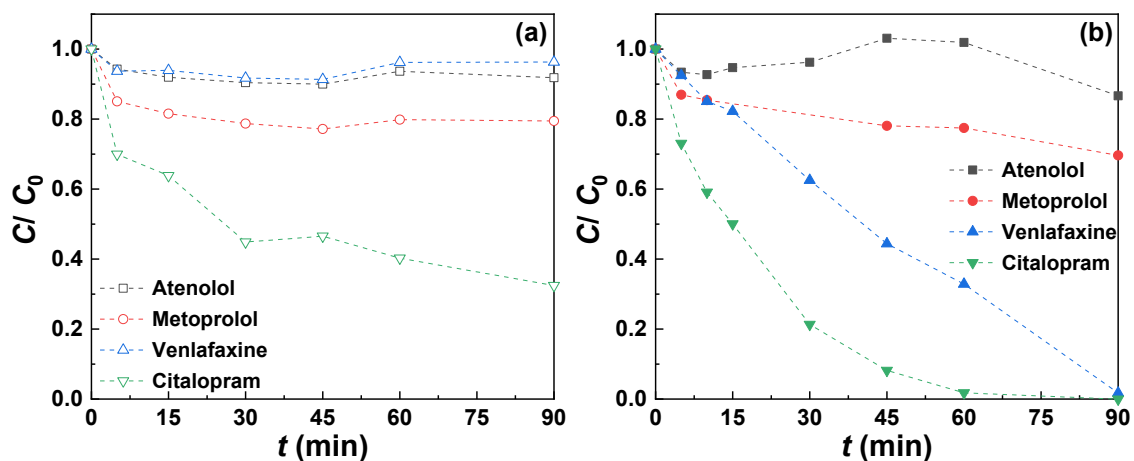
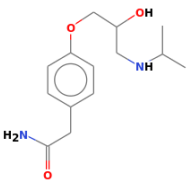
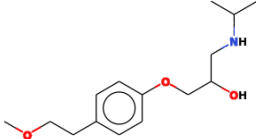
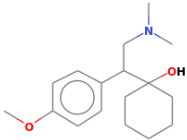
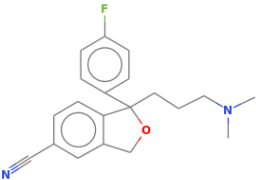


Figure S9. Normalized concentration of atenolol, metoprolol, venlafaxine, and citalopram obtained as function of time in (a) adsorption and (b) activated persulfate oxidation experiments performed in ultrapure (UP) water, with CNT@Ni+Fe/Al₂O₃-cp. Experiments performed in batch mode, with $[\text{atenolol}]_0 = [\text{metoprolol}]_0 = [\text{venlafaxine}]_0 = [\text{citalopram}]_0 = 250 \mu\text{g L}^{-1}$, $[\text{CNT@Ni+Fe/Al}_2\text{O}_3\text{-cp}] = 0.05 \text{ g L}^{-1}$, $[\text{SPS}]_0 = 250 \text{ mg L}^{-1}$, $\text{pH}_0 = 5.9$ (inherent pH), and $T = 22 \pm 2 \text{ }^\circ\text{C}$.

Table S3. Main properties of the compounds employed as model system of organic micropollutants (MPs) (NIST, 2018).

Name CAS number	Molecular formula M_w	Chemical structure
Atenolol [29122-68-7]	$C_{14}H_{22}N_2O_3$ 266.34	
Metoprolol [51384-51-1]	$C_{15}H_{25}NO_3$ 267.36	
Venlafaxine [93413-69-5]	$C_{17}H_{27}NO_2$ 277.40	
Citalopram [59729-33-8]	$C_{20}H_{21}FN_2O$ 324.39	

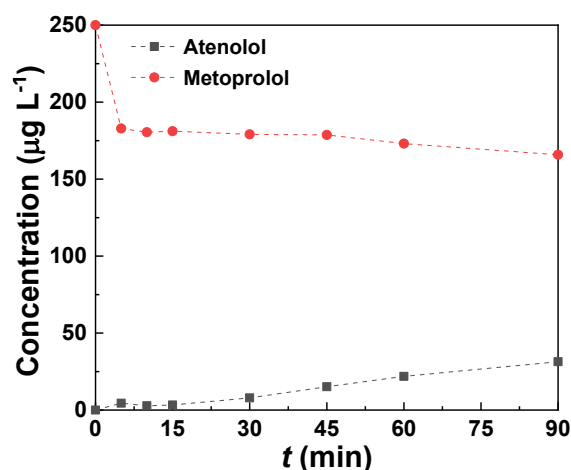


Figure S10. Evolution of metoprolol and atenolol during an activated persulfate oxidation experiment performed in ultrapure (UP) water, with CNT@Ni+Fe/Al₂O₃-cp. Experiments performed in batch mode, with [metoprolol]₀ = 250 µg L⁻¹, [atenolol]₀ = 0 µg L⁻¹, [CNT@Ni+Fe/Al₂O₃-cp] = 0.05 g L⁻¹, [SPS]₀ = 250 mg L⁻¹, pH₀ = 5.9 (inherent pH), and $T = 22 \pm 2$ °C.

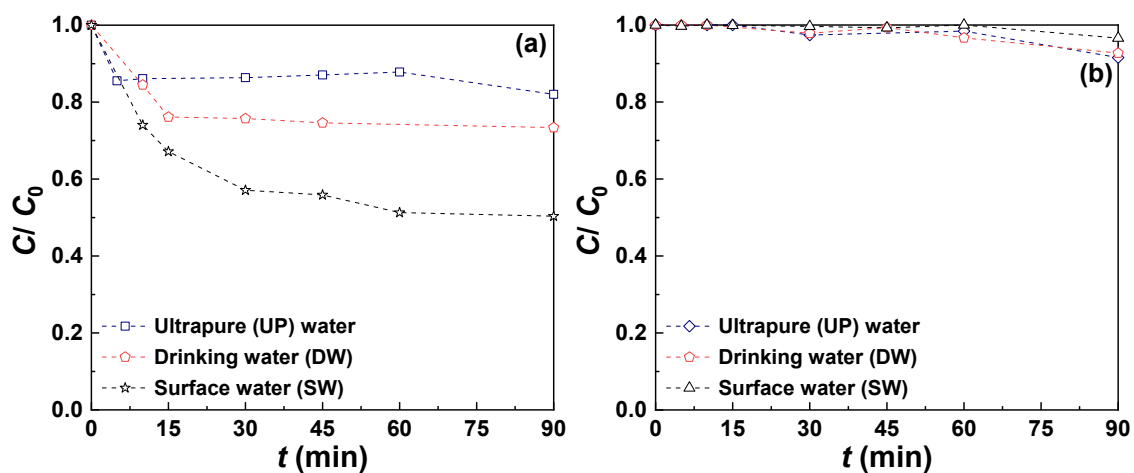


Figure S11. Normalized concentration of venlafaxine obtained as function of time in (a) adsorption experiments in the presence of CNT@Ni+Fe/Al₂O₃-cp and (b) non-catalytic experiments in the presence of SPS only. Experiments performed in batch mode, with [venlafaxine]₀ = 250 µg L⁻¹, [CNT@Ni+Fe/Al₂O₃-cp] = 0.25 g L⁻¹, [SPS]₀ = 250 mg L⁻¹, pH₀ = 5.9, 6.8 and 7.5 (inherent pH of UP water, DW and SW, respectively), and $T = 22 \pm 2$ °C.

References

NIST, 2018. National Institute of Standards and Technology (NIST), NIST Standard Reference Database 69: NIST Chemistry WebBook. U.S. Secretary of Commerce on behalf of the United States of America. <https://doi.org/10.18434/T4D303>

Vieira, O., Ribeiro, R.S., Pedrosa, M., Lado Ribeiro, A.R., Silva, A.M.T., 2020. Nitrogen-doped reduced graphene oxide – PVDF nanocomposite membrane for persulfate activation and degradation of water organic micropollutants. Chem. Eng. J. 402, 126117. <https://doi.org/10.1016/j.cej.2020.126117>

Zhao, X., Ma, J., Wang, Z., Wen, G., Jiang, J., Shi, F., Sheng, L., 2012. Hyperbranched-polymer functionalized multi-walled carbon nanotubes for poly (vinylidene fluoride) membranes: From dispersion to blended fouling-control membrane. Desalination 303, 29-38. <https://doi.org/10.1016/j.desal.2012.07.009>